Transactions on Electrical and Electronic Materials
https://doi.org/10.1007/s42341-021-00285-5

Online ISSN 2092-7592
Print ISSN 1229-7607

REGULAR PAPER

Effect of Silicon Doping on the Electrical Performance of Amorphous SiInZnO Thin-film Transistors

Byeong Hyeon Lee[1] · Dae-Hwan Kim[3] · Doo-Yong Lee[4] · Sungkyun Park[4] · Sangsig Kim[1] · Hyuck-In Kwon[3] · Sang Yeol Lee[2]

Received: 20 October 2020 / Revised: 6 January 2021 / Accepted: 15 January 2021

Abstract
The change of the electrical properties of amorphous SiInZnO thin-film transistors (SIZO TFTs) depending on Si concentration have been investigated. As the Si content increased from 1 to 3 wt%, the electrical properties are systematically degraded, such as field-effect mobility from 19.86 to 11.16 $cm^2\ V^{-1}\ s^{-1}$. This change in properties has been found to deteriorate the SIZO network when Si content is highly added. In order to analyze the change of the electrical properties of SIZO depending on Si concentration, low frequency noise method and X-ray photoelectron spectroscopy analysis are adopted to investigate trap states in energy bandgap and oxygen vacancies of SIZO system. As a result, it was found that doping with a large amount of Si destabilizes the SIZO network, resulting in degrading electrical properties.

Keywords Thin-Film transistor · Silicon doping · Low-frequency noise · X-ray photoelectron spectroscopy

1 Introduction

Since metal-oxide (MO) semiconductor based thin-film transistors (TFTs) can be applied to various fields, such as display back-plane devices, integrated circuits, and flexible devices, much research is being conducted [1, 2]. Among them, ZnO-based semiconductor materials are well known as the most famous MO semiconductors, and have a wide bandgap (> 3 eV) which are transparent in the visible region. They can be applied to various form factors because there is no limitation on the selection of substrates due to amorphous phase and low processing temperature [3, 4]. In the case of binary ZnO semiconductors, however, they conventionally show polycrystalline phases, and thus the problem of non-uniformity and instability is one of key issues [5]. Since the introduction of quaternary a-IGZO as MO semiconductor material exhibiting amorphous characteristics for the first report from Hosono *et. al.* in 2004, MO semiconductors have been steadily researching that dopant additional materials to give them an amorphous phase [6, 7]. Research on the electrical properties and the stability of materials, such as a-ITZO, a-ZTO, a-ATIZO, a-HIZO and a-SZTO, which show amorphous phase, is being conducted. Especially, changes in the electrical properties depending on the composition ratio of materials are being intensively studied [8–12]. In the case of In-based amorphous MOs, in particular, are known to exhibit high-electron mobility due to the large spherical 5 s orbital of In [13]. Therefore, IZO based MO is considered as one of the high-potential materials for active channel layer materials. However, for pure IZO semiconductor materials, it is very difficult to control the conductivity due to the high charge concentration, and instability becomes a problem under various stresses [14, 15]. Therefore, it adds additional oxygen vacancy suppressor materials, such as Ga, Hf, and Si etc., to control the carrier concentration and the stability [7, 11, 12]. Recently, many results have been reported to improve the stability of IZO semiconductors using Si, which has a strong bonding strength with oxygen [16, 17]. It has been clearly observed that oxygen vacancies can be effectively suppressed with low Si content. However, research on the case where high

✉ Sang Yeol Lee
sylee2020@gachon.ac.kr

[1] Department of Microdevice Engineering, Korea University, Seoul 136-701, South Korea

[2] Department of Electronic Engineering, Gachon University, Seongnam 13120, South Korea

[3] School of Electrical and Electronics Engineering, Chung-Ang University, Seoul 156-756, South Korea

[4] Department of Physics, Pusan National University, Busan 609-735, South Korea

Published online: 28 January 2021

content of Si is doped is still insufficient. Si atoms can effectively suppress oxygen vacancies, but it is very important to find the optimized composition ratio because it can degrade the properties of the device if added in excess.

In this study, we fabricated a-SIZO TFT with high Si content of 1 to 3 wt.% to observe the change of the electrical properties. In addition, low-frequency noise (LFN) as a physical analysis method and X-ray photoelectron spectroscopy (XPS) as a chemical analysis method were used to effectively analyze the change of defect states depending on the Si content. Systematic analysis of this effective change depending on Si content is very important evidence for effective active layer design.

2 Experimental Details

Before the deposition, the substrate (heavily boron doped p^+-type Si substrate with 200-nm SiO_2 deposited by thermal oxidation was used with a resistivity of 0.001–0.002 $\Omega \cdot cm^{-1}$) was cleaned in acetone, methanol, and de-ionized water for 10 min each in ultrasonication bath. The a-SIZO ceramic target was fabricated by high purity powder mixtures of SiO_2, In_2O_3, and ZnO. In order to observe the properties according to the Si content, the ratio of In_2O_3 and ZnO was fixed to 3:1 and then the Si content was changed from 1 to 3 wt.% with active channel layer thickness of 23 nm. The a-SIZO thin films depending on Si content were fabricated at room temperature using RF magnetron sputtering system. The sputtering conditions are as follows: sputter power of 30 W, gas flow rate of $Ar:O_2 = 30:0$ sccm, and deposition pressure of 2 mTorr,. Next, the channel layers were patterned using the conventional photolithography and wet-etching processes. After patterned, annealing was performed in an air atmosphere at 150 °C for 2 h using a furnace. The source/drain electrodes were deposited with 10 nm and 40 nm of titanium (10 nm) and aluminum (50 nm) using E-beam/thermal evaporator, respectively. The width/length of the channel of fabricated TFTs are 50 µm/50 µm, respectively.

The electrical characteristics of a-SIZO TFTs were measured using a semiconductor parameter analyzer (HP 4145B, Hewlett-Packard Co.) in a vacuum probe station (vacuum state of < 2.67 Pa). The atomic ratio and O1s peaks of the thin films were measured using XPS, and fitting was performed using the Gaussian–Lorentzian method. The XPS measurements were performed after surface etching to characterize pure SIZO films. The noise measurements were conducted using an Agilent 89,441 vector-signal analyzer with an SR570 low-noise current amplifier.

3 Results and Discussion

Figure 1a and b show the cross-sectional transmission electron microscopy (TEM) image and energy dispersive spectromery (EDS) of the fabricated 1SIZO TFT. Based on the TEM results, the thicknesses of the deposited SIZO, Ti, and Al are clearly observed to be 23 nm, 10 nm, and 50 nm, respectively. In addition, the Pt layer is an additional layer to facilitate the TEM analysis. It is observed that each layer is very clearly separated, and no additional oxidation was found in the metal layer. This is further confirmed through elemental analysis as shown in Fig. 1b. According to the EDS mapping results, each element is identified by the following color: Si of green, Zn of blue, In of purple, O of red, Ti of sky-blue, Al of pink, and Pt of yellow. Each element is clearly observed to be well separated and deposited at the selected location without additional diffusion mainly due to room temperature process. The transfer characteristic of the SIZO TFT depending on the Si content at $V_{DS} = 0.1$ V is shown in Fig. 1c. Furthermore, the electrical properties, such as field-effect mobility (μ_{fe}), threshold voltage (V_{th}) measured at $I_D = 1$ nA, on/off current ratio ($I_{on/off}$), and subthreshold swing (SS), were summarized in Table 1. As the Si ratio rapidly increased from 1 wt.% to 3 wt.%, the V_{th} shifted in positive direction from -4.67 V to 0.95 V, and the $I_{on/off}$, systematically decreased while increasing SS value. It is clearly observed that excessive Si atoms damage the IZO system. Since Si has a high bonding strength with oxygen, so it was confirmed that additional defects caused by excess oxygen or Si atom. It is also important to note that, in the case of μ_{fe}, a sharp decrease from 19.86 $cm^2\ V^{-1}\ s^{-1}$ to 11.16 $cm^2\ V^{-1}\ s^{-1}$ was clearly observed. The μ_{fe} is given by:

$$\mu_{fe} = \frac{L\ g_m}{W\ V_{DS}\ C_{ox}}, \tag{1}$$

where V_{DS} is the drain to source voltage, C_{OX} is the gate capacitance of dielectric, g_m is the trans-conductance, L and W denote the active channel length and width, respectively [17]. In our previous results, we analyzed that the electrical properties, such as μ_{fe}, V_{th}, and $I_{on/off}$ are changed as increasing the Si content even in the case of containing a small amount of Si atom. It was analyzed that this occurred due to the decrease of the carrier concentration because the Si had a strong bonding strength with oxygen (799.6 kJ/mol) to suppress the formation of oxygen vacancies [12, 16]. However, in this paper in the case of high Si content included, the opposite trend of not decreasing SS value was observed. In general, the SS value is closely related to the interface defect state (N_{IT}) [18]. In addition, in the case of TFTs, there are many reports that the defect state of the active channel layer also affects the SS value [19]. Since this would significantly reduce the quality of the thin film if the Si content was too

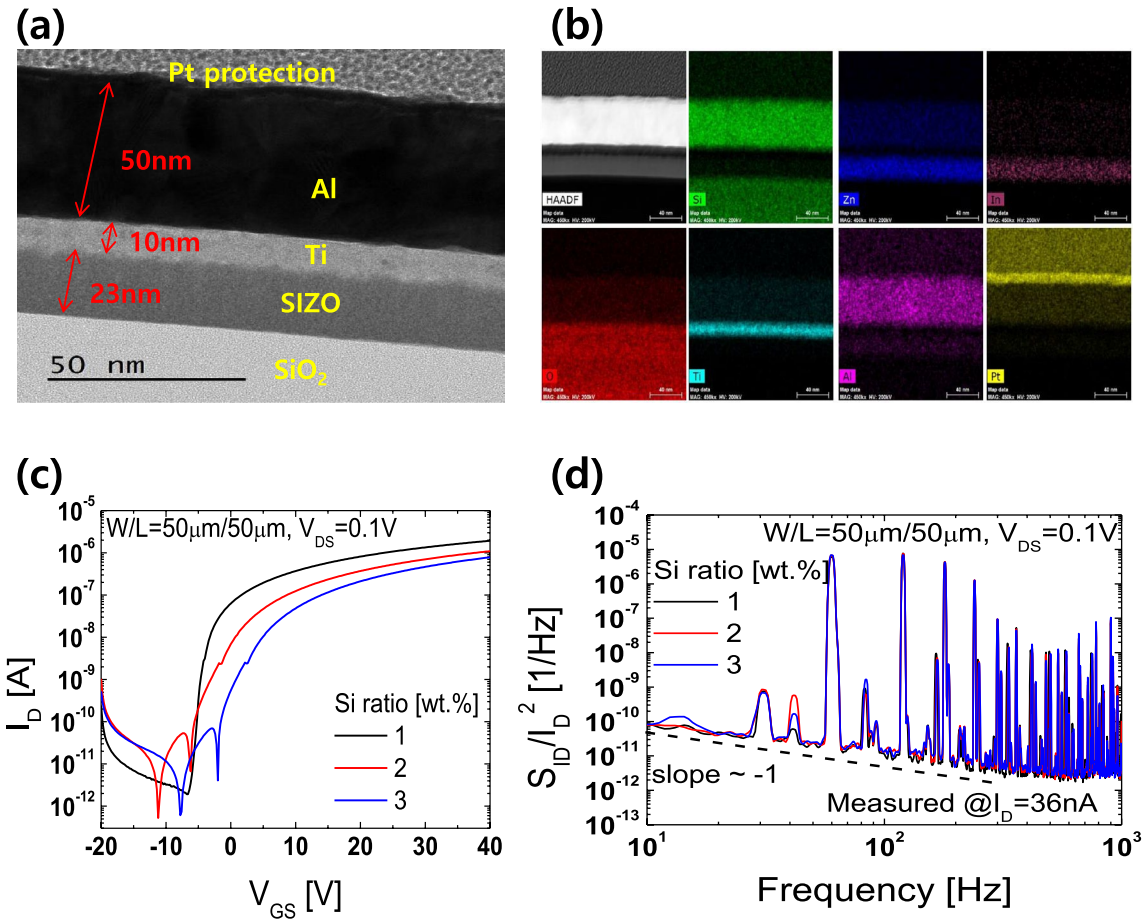

Fig. 1 **a** Cross-section TEM image of 1SIZO TFT, **b** EDS mapping image: green Si atom, blue Zn atom, purple In atom, red oxygen atom, sky-blue Ti atom, pink Al atom, and yellow Pt atom, **c** transfer characteristic of a-SIZO TFTs, and **d** normalized noise power spectral density of a-SIZO TFTs as function of Si content

Table 1 Electrical characteristics of a-SIZO TFTs depending on Si content

Sample	V_{th} (V)	I_{on} (A)	I_{off} (A)	$I_{on/off}$	μ_{fe} (cm^2 V^{-1} s^{-1})	SS (V decade^{-1})
1SIZO	−4.67	1.9×10^{-6}	1.9×10^{-12}	1.0×10^{6}	19.86	0.53
2SIZO	−2.91	1.1×10^{-6}	1.6×10^{-11}	7.8×10^{4}	13.05	1.18
3SIZO	0.95	7.8×10^{-7}	1.8×10^{-11}	4.3×10^{4}	11.16	1.19

high, we have conducted LFN analysis to verify the effect of Si on the change of defect states. Figure 1d depicts the normalized noise power spectral density (S_{ID}/I_D^2) versus frequency from 10 Hz to 1 kHz of the SIZO TFTs depending to the Si content. The difference of S_{ID}/I_D^2 with the change of Si content was hardly seen. However, it has been confirmed that noise depending on the frequency has severe fluctuation as increasing Si content. The graph shows the pure $1/f^{\gamma}$ with frequency exponent γ is close to 1. From the previous work, LFN characteristic in TFTs can be analyzed by three models: the mobility fluctuation ($\Delta\mu$) model, the carrier number fluctuation (Δn) model, and the correlated number fluctuation-mobility fluctuation (Δn-$\Delta\mu$) model [20–22]. In order to analyze the main mechanism caused by LFN in the TFTs, it is necessary to compare the effects on S_{ID}/I_D^2 versus I_D at a fixed frequency. The symbols in Fig. 2a–c show the experimentally measured S_{ID}/I_D^2 versus I_D at a fixed frequency of 10 Hz. The slope of SIZO TFTs depending on Si content shows Δn-$\Delta\mu$ model, and S_{ID}/I_D^2 upswing at high I_D region explained the LFN generated by the series resistance [23]. According to the Δn-$\Delta\mu$ model, S_{ID}/I_D^2 can be expressed as following [23]:

$$\frac{S_{ID}(f)}{I_{ds}^2} = \left[1 + \alpha_S \mu_{fe} C_{OX} \frac{I_{ds}}{g_m}\right]^2 \left[\frac{g_m}{I_{ds}}\right]^2 S_{VFB}, \quad (2)$$

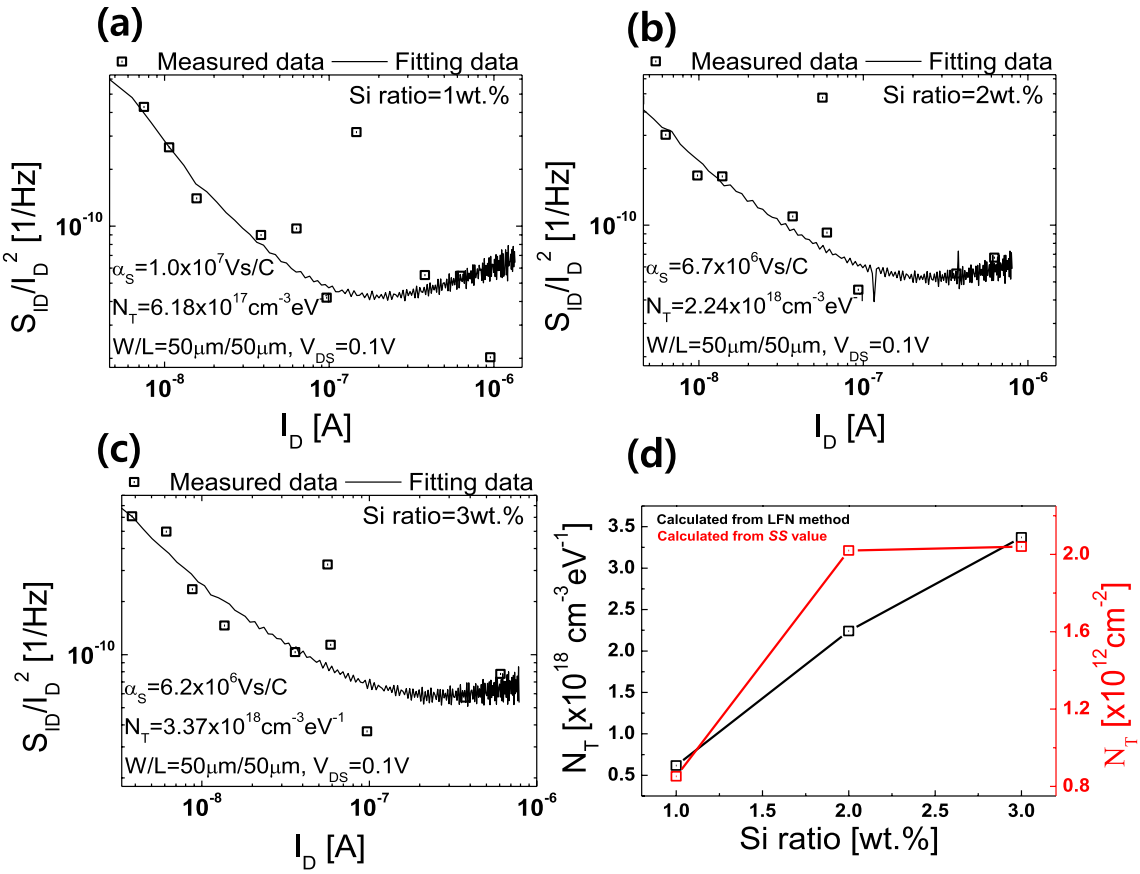

Fig. 2 Normalized noise power spectral density versus drain current at fixed frequency of 10 Hz in **a** 1SIZO, **b** 2SIZO, and **c** 3SIZO TFTs. **d** Calculated N_T value from LFN method (black) and *SS* value (red)

$$S_{VFB} = \frac{q^2 kTN_T\lambda}{WLC_i^2 f}, \tag{3}$$

where S_{VFB} is the flat-band voltage noise spectral density, α_s is the Coulomb scattering coefficient, q is the elementary charge, T is the temperature, g_m is the trans-conductance, k is the Boltzmann constant, C_{OX} is the dielectric capacitance per unit area, N_T is the near interface trap density, and λ is the tunneling attenuation distance (~0.1 nm in SiO_2). Using Eqs. (2) and (3) we can get the solid fitting line as shown in Fig. 2a–c. As a result, the SIZO TFT depending on the Si content can be clearly interpreted by the Δn-$\Delta\mu$ model. In addition, the N_T value extracted by the LFN method (black line) and the N_T value extracted by the *SS* value (red line) are shown in Fig. 2d. We extracted the N_T value from *SS* value by the following equation [19]:

$$N_T = \left(\frac{SSlog(e)}{\frac{kT}{q}} - 1\right)\frac{C_{ox}}{q} \tag{4}$$

herein, *SS* is the subthreshold slope, k is the Boltzmann's constant, T is the temperature, and C_{ox} is the dielectric capacitance. It can be clearly observed that N_T extracted by both methods shows the same trend. As the Si content increased, N_T extracted by LFN method increased from 6.18×10^{17} cm^{-3} eV to 3.37×10^{18} cm^{-3} eV, and N_T extracted by *SS* value increased systematically from 8.52×10^{11} cm^{-2} to 2.04×10^{12} cm^{-2}. It was clearly observed that this trend differs from the stability improvement through the suppression of the oxygen vacancies our previously reported as mention above. In the case of a small amount of Si, oxygen tends to be suppressed and stability to be improved. However, in the case of SIZO to which a large amount of Si is added, the electrical characteristics have been changed due to the increased trap state inside the active channel layer. In addition, we used XPS to analyze the effects of large amounts of Si on SIZO systems. The measurement was performed after the surface was etched to eliminate the impurity caused by the thin film surface before XPS analysis.

Figure 3 shows atomic ratios of elements at the SIZO thin films depending on Si content. The atomic ratios of

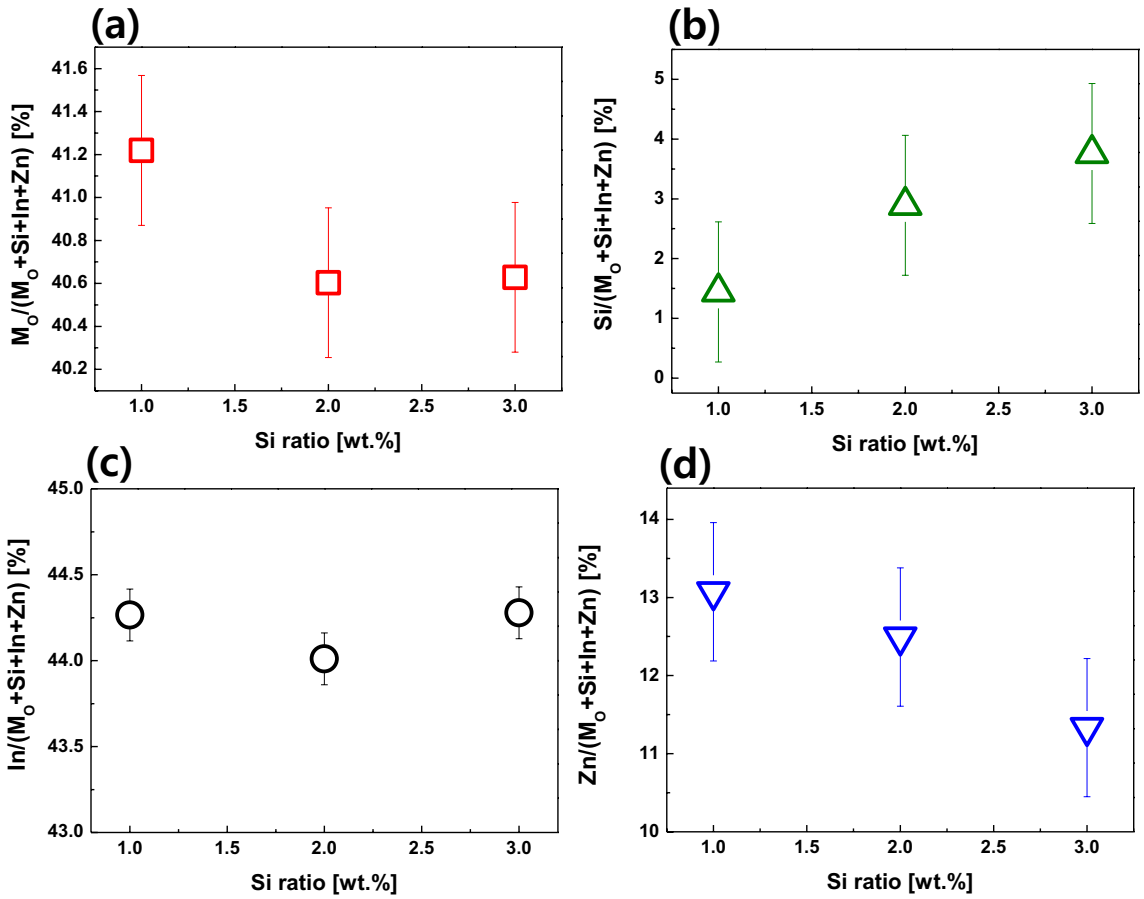

Fig. 3 Atomic ratio of SIZO thin films depending on Si content **a** M–O, **b** Si, **c** In, and **d** Zn, respectively

each elements were calculated from XPS intensities as following equation [24]:

$$\text{Atomic ratio (\%)} = \frac{\frac{I_X}{F_X}}{\frac{I_{M_O}}{F_{M_O}} + \frac{I_{Si}}{F_{Si}} + \frac{I_{In}}{F_{In}} + \frac{I_{Zn}}{F_{Zn}}} \quad (5)$$

where X denotes the elements in SIZO, such as metal-oxide (M_O), Si, In, and Zn, F the atomic sensitivity factors, and I is the total XPS peak area of individual emission from elements. According to the atomic ratio results, it was confirmed that the content of Si atoms clearly increased with increasing Si content. Interestingly, it was found that the In ratio hardly changed, but the ratio of M_O and Zn decreased relatively. In general, Zn is well known as network former in ZnO-based MO materials 25 Therefore, it is confirmed that as the Si content increases, the MO network is deteriorated.

Figure 4a–c show the XPS data of SIZO depending on Si content which indicate that the core-level spectra of O 1 s peak. The binding energy of O 1 s peaks were calibrated by taking C 1 s reference at 284.50 eV. The O 1 s peak can be deconvoluted into three peaks with Gaussian–Lorentzian functions for the quantitative analysis. The lower binding energy (O_I), which occurs at 530 ± 0.3 eV, associated with the metal-oxide bonding. The middle binding energy (O_{II}) observed at 531 ± 0.3 eV. This O_{II} peak can be attributed to oxygen-vacancy in active channel layer as SIZO. The higher binding energy (O_{III}) at 532.2 ± 0.3 eV is closely related with the surface oxygen [26]. From the O 1 s peak, we observe how the three deconvoluted peaks mentioned above change with increasing Si content as summarized in Fig. 4d. As the Si content increases, the proportion of O_{III} peak has not been changed around 12%. Since the surface is etched, so it has a very clean surface. On the other hand, O_{II} peaks show a systematic increase from 25.6 to 30.1% as increasing Si content. This is because the presence of a large amount of Si atoms destabilizes the MO bonds, thus creating more oxygen vacancies. In addition, the O_I peak showed a tendency to decrease systematically as mentioned above from 61.7 to 57.9% as the Si content increased. It is clearly observed that for SIZO containing high Si atoms, the increase in defects and the formation of MO networks are hindered. Therefore, when Si is added in IZO system, it should be

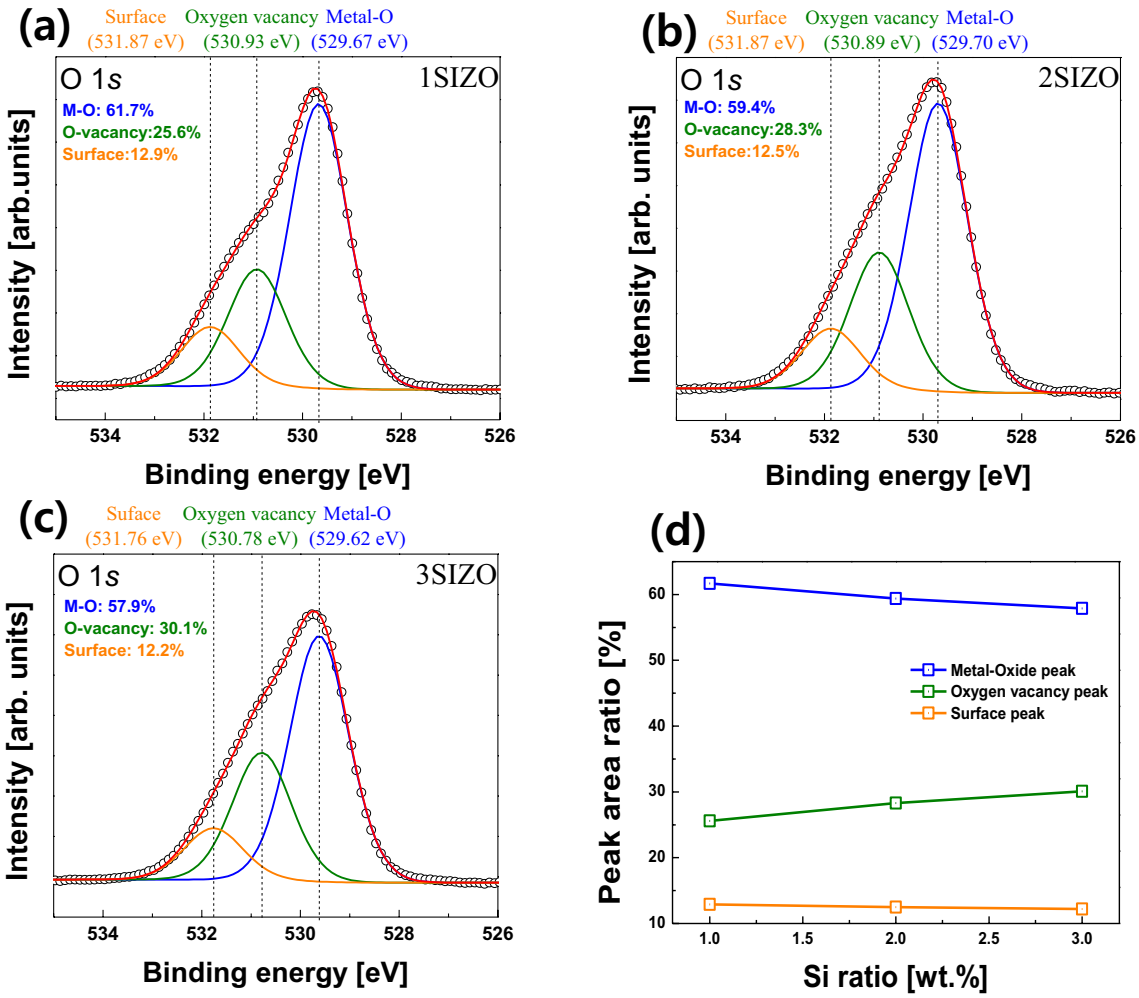

Fig. 4 X-ray photoelectron spectroscopy spectra of O 1 s peak of a-SIZO thin films depending on Si content: **a** 1SIZO, **b** 2SIZO, **c** 3SIZO. **d** Summarized peak ratio of a-SIZO thin films as function of Si content

designed to be optimized by considering the content to obtain high electrical characteristics and stability.

4 Conclusion

In summary, we have characterized the SIZO thin films doped with high concentrations of Si using the LFN method, as the physical analysis method, and the XPS, as the chemical analysis method. From the LFN results, we found that the SIZO TFT according to the Si content is in good agreement with the Δn-$\Delta\mu$ model. Furthermore, N_T values extracted by the LFN method and N_T extracted by the *SS* value showed the same tendency to increase systematically as the Si content increased. In XPS O 1 s results, O_I peak ratio decreased and O_{II} peak ratio increased with increasing Si content. Contrary to the reduction of oxygen vacancies, which appeared when Si was doped at low concentrations, it was clearly observed that at high concentration of Si, the SIZO TFT properties are deteriorated. As a result, when designing a highly stable TFT, it is very important to determine the optimized Si content on the IZO system.

References

1. D.-C. Hays, B.P. Gila, S.J. Pearton, F. Ren, Appl. Phys. Rev. **4**, 021301 (2017)
2. L. Petti, N. Munzenrieder, C. Vogt, H. Faber, L. Buthe, G. Cantarella, F. Bottacchi, T.-D. Anthopoulos, G. Troster, Appl. Phy. Rev. **3**, 021303 (2016)
3. R.L. Hoffman, B.J. Norris, J.F. Wager, Appl. Phys. Lett. **82**, 733 (2003)
4. E. Fortunato, P. Barquinha, A. Pimentel, L. Pereira, G. Goncalves, R. Martins, Phys. Status Solidi Rapid Res. Lett. **1**, 1 (2007)
5. J.S. Park, W.-J. Maeng, H.-S. Kim, J.S. Park, Thin Solid Films **520**, 1679 (2012)

6. K. Nomura, H. Ohta, A. Takagi, T. Kamiya, M. Hirano, H. Hosono, Nature (London) **432**, 488 (2004)
7. H. Hosono, J. Non-Cryst, Solids **352**, 851 (2006)
8. R.N. Bukke, C. Avis, M.N. Naik, J. Jang, IEEE Electron Device Lett. **39**, 371 (2018)
9. H.Q. Chiang, J.F. Wager, R.L. Hoffman, J. Jeong, D.A. Keszler, Appl. Phys. Lett. **86**, 013503 (2005)
10. S. Yang, D.H. Cho, M.K. Ryu, S.H.K. Park, C.S. Hwang, J. Jang, J.K. Jeong, IEEE Electr. Device Lett. **31**, 144 (2009)
11. E. Chong, K.C. Jo, S.Y. Lee, Appl. Phys. Lett. **96**, 152102 (2010)
12. B.H. Lee, A. Sohn, S. Kim, S.Y. Lee, Sci. Rep. **9**, 886 (2019)
13. T. Kamiya, K. Nomura, H. Hosono, J. Disp. Technol. **5**, 273 (2009)
14. P. Xiao, T. Dong, L. Lan, Z. Lin, W. Song, D. Luo, M. Xu, J. Peng, Sci. Rep. **6**, 25000 (2016)
15. D.-C. Paine, B. Yaglioglu, Z. Beiley, S. Lee, Thin Solid Films **516**, 5894 (2008)
16. J.Y. Choi, K. Heo, K.S. Cho, S.W. Hwang, J. Chung, S. Kim, B.H. Lee, S.Y. Lee, Sci. Rep. **7**(1), 1–8 (2017)
17. J.Y. Choi, S. Kim, B.-U. Hwang, N.-E. Lee, S.Y. Lee, Semicond. Sci. Technol. **31**, 125007 (2016)
18. Z. Yang, J. Yang, T. Meng, M. Qu, Q. Zhang, Mater. Lett. **166**, 46 (2016)
19. B.H. Lee, S.Y. Lee, Phys. Status Solidi A **215**, 1700698 (2018)
20. F.N. Hooge, IEEE Trans. Electron Devices **41**, 1926 (1994)
21. H.-J. Kim, C.-Y. Jeong, S.-D. Bae, H.-I. Kwon, J. Vac. Sci. Technol. B **35**, 010601 (2017)
22. K.K. Hung, P.K. Ko, C. Hu, Y.C. Cheng, IEEE Trans. Electron Devices **37**, 654 (1990)
23. C.Y. Jeong, H.J. Kim, D.H. Kim, H.S. Kim, E.S. Kim, T.S. Kim, J.S. Park, J.B. Seon, K.S. Son, S. Lee, S.H. Cho, IEEE Electron. Device Lett. **37**, 739–742 (2016)
24. T. Weiss, J. Warneke, V. Zielasek, P. Swiderek, M. Baumer, J. Vac. Sci. Technol. A **34**, 041515 (2016)
25. T. Kamiya, M. Kawasaki, MRS bull **33**, 1061 (2008)
26. B.H. Lee, D.-Y. Lee, A. Sohn, S. Park, D.-W. Kim, S.Y. Lee, J. Alloy. Compd. **715**, 9 (2017)